Molecular Electronics

DOI: 10.1002/anie.201406223

Electrical Network of Single-Crystalline Metal Oxide Nanoclusters Wired by π-Molecules**

Ryo Tsunashima, Yoshifumi Iwamoto, Yusuke Baba, Chisato Kato, Katsuya Ichihashi, Sadafumi Nishihara, Katsuya Inoue, Katsuya Ishiguro, Yu-Fei Song, and Tomoyuki Akutagawa*

Abstract: *In a mixed-valence polyoxometalate, electrons are usually delocalized within the cluster anion because of low level of inter-cluster interaction. Herein, we report the structure and electrical properties of a single crystal in which mixed-valence polyoxometalates were electrically wired by cationic π-molecules of tetrathiafulvalene substituted with pyridinium. Electron-transport characteristics are suggested to represent electron hopping through strong interactions between cluster and cationic π-molecules.*

Polyoxometalates (POMs) are anionic metal oxide molecules. They are finite frameworks composed of a transition metal M (assumed in this case to be Mo or W) bridged through oxo ligands, which results in metal oxide nanoclusters with the diversities of cluster morphology, size, and composition.[1] Since M exists at a high oxidation state of +6 (Mo^{VI} and W^{VI}), the cluster anion is easily reduced, giving stable mixed-valence states between M^{V} and M^{VI}. Usually, an added electron (sometimes called a "blue electron" because it imparts a blue color to the reduced POM cluster) is trapped in a single cluster and delocalized over several M sites with low activation energy.[2] Unique cluster shapes, for example, wheel, lemon, cube, and capsule, with 1–5 nm cluster diameters have attracted attention for establishing unprecedented electrical properties for future molecular electronics. For example, switching of the exchange interactions between two electron spins have been proposed using the $\{PMo_{12}O_{40}(VO)_2\}$ anion.[3] The anion consists of a mixed valence $\{PMo_{12}O_{40}\}$ Keggin unit capped with two vanadyl groups containing two localized spins. Another example is the $\{(SO_3)_2Mo_{18}O_{54}\}$ anion, which shows a temperature-induced reversible electron-transfer transition within a single cluster.[4] Further developments can be expected by concerted efforts between materials design and exploration; however, an intrinsic issue remains, that is, effecting electrical connections between POM clusters in the crystalline solid. Electron systems are strongly isolated within a single cluster because of low level of inter-cluster interaction. As such, an electrical network of POMs has only been achieved using a nanogap electrode.[5]

Herein, we focus on cationic π-conjugating molecules as a means of facilitating electron transport through POM clusters in a solid. Of the possible cationic π-conjugating molecules, we employed an electron donor of tetrathiafulvalene (TTF)[6] substituted with pyridinium (TTFPyH), giving cationic characteristics that enable the formation of a salt with anionic POMs. Even though a variety of hybrids between POMs and TTF analogies have been explored, the intermolecular interactions between POM and TTF analogies have usually been low. At present, electronic transport has only been observed in a π-column constructed of a TTF moiety with POM clusters almost electronically isolated from the conduction column.[6e–h]

In contrast, herein we report the structure and electrical properties of a single crystal of $(TTF^{+}PyH^{+})_2[PMo^{V}Mo^{VI}_{11}O_{40}]\cdot n H_2O$ (**1**), where n is the number of crystalline water molecules associated with the structure. In the crystal, protonated $TTF^{+}PyH^{+}$ ions form salts with Mo-based Keggin clusters. As a result of the higher electron withdrawing ability of $[PMo^{VI}_{12}O_{40}]^{3-}$, a redox reaction between TTFPy and the cluster anion results in reduction to a mixed-valence state of $[PMo^{V}Mo^{VI}_{11}O_{40}]^{4-}$ and oxidation to $TTF^{+}PyH^{+}$ in crystal **1**. The TTF moiety did not employ the π-column. Instead, extended interactions were observed between $TTF^{+}PyH^{+}$ and $[PMo^{V}Mo^{VI}_{11}O_{40}]^{4-}$ molecules with alternative packing. Semiconducting behavior was observed with an activation energy of approximately 0.4 eV, and conduction was suggested to originate from electron hopping in extended networks.

Figure 1 shows the packing structure of crystal **1**. Oxidized and protonated $TTF^{+}PyH^{+}$ molecules form a dimer structure with intermolecular atomic S···S distances of 3.323(5) Å

[*] Dr. R. Tsunashima, Prof. K. Ishiguro
Graduate School of Science and Engineering
Yamaguchi University
Yoshida 1677-1, Yamaguchi, 753 8512 (Japan)
E-mail: ryotsuna@yamaguchi-u.ac.jp
Y. Iwamoto, Y. Baba
Department of Biology and Chemistry, Yamaguchi University
Yoshida 1677-1, Yamaguchi, 753 8512 (Japan)
C. Kato, K. Ichihashi, Dr. S. Nishihara, Prof. K. Inoue
Graduate School of Science, Hiroshima University
1-3-1 Kagamiyama, Higashi-Hiroshima 739-8526 (Japan)
Dr. S. Nishihara, Prof. K. Inoue
Institute for Advanced Materials Research, Hiroshima University
Higashi-Hiroshima 739-8530 (Japan)
Prof. Y.-F. Song
State Key Laboratory of Chemical Resource Engineering, Beijing University of Chemical Technology
100029 Beijing (P. R. China)
Prof. T. Akutagawa
Institute of Multidisciplinary Research for Advanced Materials (IMRAM), Tohoku University
Sendai 980-8577 (Japan)

[**] This work was partly supported by the cooperative research program of the Network Joint Research Centre for Materials and Devices of Japan and Grant-in-Aid for Science Research from the Ministry of Education, Culture, Sports, Science and Technology of Japan.

Supporting information for this article is available on the WWW under http://dx.doi.org/10.1002/anie.201406223.

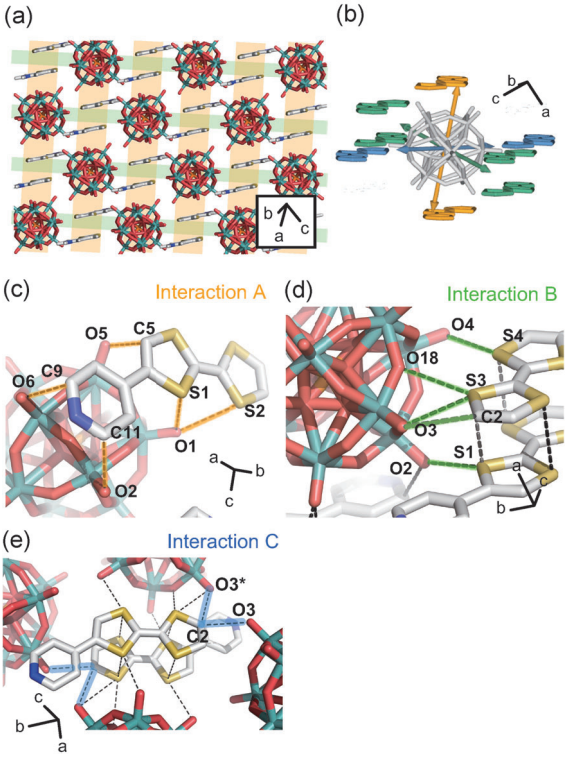

Figure 1. Molecular and packing structure of the single crystal of **1**. a) Structure in the (011) plane orange and green bands represent the directions of interactions A and B, respectively. b) Intermolecular interactions A–C of $\{PMo_{12}\}$ clusters. Orange, green, and blue arrows represent the directions of interactions A, B, and C, respectively. These interactions are also shown in detail in (c)–(e), respectively. Dashed lines represent interactions where interatomic distances are shorter than those that are the sum of van der Waals radii (interactions A–C are colored). Interatomic distances [Å]: for interaction A: O2···C11 3.10(2), O6···C9 2.98(2), O5···C5 3.004 (16), O1···S1 3.179(11), O1···S2 3.303(8). For interaction B: O4···S4 3.118(8), O18···S3 3.150(8), O3···S3 3.264 (8), O3···C2 3.107(12), O2···S1 3.056(6). For interaction C: O3···C2 3.076(16) O3*···C2 3.107(12).

(S1···S3) and 3.418(6) Å (S2···S4), and the dimers were isolated by the $[PMo^{V}Mo^{VI}_{11}O_{40}]^{4-}$ cluster anion. Similar dimers of eclipsed TTF stacks were observed for (TTF)Br, and the highest intermolecular overlapping was expected between TTF molecules in this form.[7] The $[PMo^{V}Mo^{VI}_{11}O_{40}]^{4-}$ cluster interacted with $TTF^{+}PyH^{+}$ through O···S and O···C interactions (Figure 1 b), and they were categorized into three main types of interactions A, B, and C (Figure 1 b–e). Type A represented an interaction along the $a-b+c$ direction and type B represented an interaction along the $a+b-c$ direction as a result of face-to-face and side-by-side configurations between cluster and dimer, respectively, forming two dimensional networks in the (011) plane. In addition to these, intermolecular interaction was observed between C2 and O3 (type C interaction), and these interactions pillared a two dimensional sheet.

The oxidation state of the TTF moiety in **1** was estimated from bond-length considerations and confirmed by Fourier transform infrared (FT-IR) spectra. Bond lengths of the TTF moiety are usually a function of its oxidation state.[8] We estimated the charge of the TTF moiety to approximately +1 (Figure S4-2 in the Supporting Information), yielding a $TTF^{+}PyH^{+}$ cation. The TTF moiety was oxidized and formed a dimer structure. A similar radical dimer has been observed for TTF.[7] Upon oxidation of TTF, the FT-IR peak of the central C=C vibration has been shown to exhibit a shift from 1530 to 1471 cm^{-1}.[9] The C=C vibration in crystal **1** was observed at 1472 cm^{-1}, which was shifted from 1553 cm^{-1} by TTFPy (Figure S2-2).

The corresponding electron acceptor was $\{PMo_{12}\}$. The temperature-dependent magnetic susceptibility showed paramagnetic behavior where the Currie constant was found to be 0.364 emu K mol^{-1}, which indicates the existence of a spin ($S=1/2$) on $[PMo^{V}Mo^{VI}_{11}O_{40}]^{4-}$. The composition and electronic state of **1** was deduced to be $(TTFPyH)_2[PMo^{V}Mo^{VI}_{11}O_{40}]$ with several numbers of crystalline water molecules.

Figure 2 shows a plot of the temperature-dependent conductivity measured in the range 170–330 K using single-crystal material. The measurement was performed along a direction that nearly corresponded to the two-dimensional sheet of the (011) plane, that is, parallel to the *a* axis

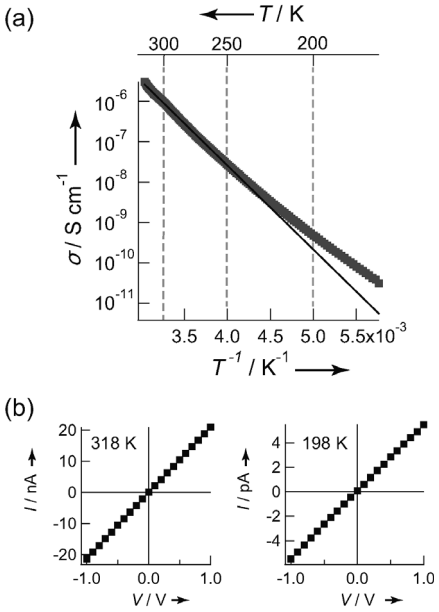

Figure 2. a) Temperature dependence of the electrical conductivity plotted with respect to T^{-1} measured using single crystals of **1**. b) Plots of *I*–*V* characteristics at 318 and 198 K. The temperature-dependent electrical conductivity obeys Arrhenius type dependence above 250 K with an activation energy of 0.42 eV.

(Figure S3-2 and S4-3). Ohmic current–voltage (*I*–*V*) characteristics were observed at each measurement point, and the conductivity showed semiconducting behavior. The electrical conductivity at 300 K was 6.30×10^{-7} S cm^{-1}. The value was still lower than that observed for TTF–POM hybrids in which the TTF moiety forms a π-conducting column ($\sigma_{RT}>10^{-4}$ S cm^{-1}, characterized using single crystals).[6e–h] We note that crystal **1** does not contain this column. TTFPy dimers interacted only with $[PMo^{V}Mo^{VI}_{11}O_{40}]^{4-}$ clusters through the intermolecular interactions shown in Figure 1.

TTFPy interacted with the O atoms of $[PMo^{V}Mo^{VI}_{11}O_{40}]^{4-}$ through interactions A and B in the (011) plane. However, the oxo ligands usually contributed to the occupied orbitals of the cluster anions and their energy level is too low to form a band-like electronic structure with TTFPy.[10] Therefore, the only possible conduction mechanism in the single crystal is thermally activated electron hopping though overlapping orbitals. Conducting electrons travel in the single crystal by hopping between the regular arrays of $[PMo^{V}Mo^{VI}_{11}O_{40}]^{4-}$ linked by the $TTF^{+}PyH^{+}$ dimers. The AC (alternative current) conductivity (σ_{AC}) for hopping conduction is established to obey a power law with respect to frequency, $\sigma_{AC} = A\omega^{s}$ (where ω and s are the angular frequency and exponent, respectively), in the intermediate frequency range (kHz). The exponent s is normally in the range of 0.6–1.[11] Crystal **1** exhibited a similar power law above 100 kHz with a slightly smaller s value of 0.5, suggesting a hopping conduction mechanism (Figure S3-5). Below 250 K, the conductivity showed a deviation from the T^{-1} plot. Deviation from an Arrhenius type behavior at low temperature has been reported in nanoparticle assemblies with electron transport often following a variable range hopping (VRH) behavior.[12] For example, an electron-transport mechanism using Mott's VRH model has been reported for a nanoparticle assembly of mixed-valence tungsten oxide.[13] Corresponding conductivity measurements along the $b+c$ axis resulted in a similar conductivity and temperature dependence. Low anisotropic conduction was considered to originate from possible electron hopping along the $b+c$ direction by interaction C.

The electrical conductivity of **1** is still low at $10^{-7}\,S\,cm^{-1}$. However, the value is higher by four orders of magnitude than that of a tetrabutylammonium salt of $[PMo_{12}O_{40}]^{3-}$, which exhibited a conductivity below the measurement range (i.e., a current at 1 V lower than 10 pA, corresponding to a conductivity below $10^{-11}\,S\,cm^{-1}$). The strong interaction between $TTF^{+}PyH^{+}$ and $[PMo^{V}Mo^{VI}_{11}O_{40}]^{4-}$ is considered to enhance the conductivity. In addition, a delocalized electron in $[PMo^{V}Mo^{VI}_{11}O_{40}]^{4-}$ would also contribute to the conductivity. Further details on the conduction mechanism are currently under study and will be reported in the future.

In summary, single crystalline **1** was prepared by a redox-driven assembly between TTFPy and $[PMo^{VI}_{12}O_{40}]^{3-}$. Regular arrays of mixed-valence $[PMo^{V}Mo^{VI}_{11}O_{40}]^{4-}$ nanoclusters were observed in a single crystal, and they were electrically wired by $TTFPy^{+}H^{+}$ dimers. The electrical conductivity of the single crystal decreased toward low temperatures, while its semiconducting characteristics obeyed an Arrhenius type behavior above 250 K. The electron-transport characteristics in the crystal were suggested to represent electron hopping between $[PMo^{V}Mo^{VI}_{11}O_{40}]^{4-}$ clusters and $TTFPy^{+}H^{+}$ dimers. Usually, electrons are delocalized within a single POM cluster in a bulk solid. However, our results show that interactions with $TTFPy^{+}H^{+}$ molecules enable electron transport through POM clusters. Further development is expected by considering a similar network structure using POM clusters that exhibit electrical switching. In addition, we also note that the assembly network structure of colloidal nanoparticles are considered as promising candidates for future molecular electronics applications.[12] Highly ordered networks are expected using mixed-valence POMs, crystallizable nanoparticles, or quantum dots.

Experimental Section

TTFPy was synthesized according to the literature method.[14] Commercially available $Na_3[PMo_{12}O_{40}]$ hydrate was used without further purification. Single crystals of **1** were prepared by slow diffusion. First, an aqueous solution of $Na_3[PMo_{12}O_{40}]$ (0.8 mL of 2.2 mM) was added into a glass tube, followed by the layering of 0.8 mL quantities of water/acetonitrile mixed solvent (1:1), followed by the TTFPy solution (0.8 mL of 0.9 mM solution in acetonitrile). After 5 days of slow diffusion, blue crystals of **1** were obtained. We confirmed that at least two types of crystals were obtained having different crystal structures of cuboid (majority) and plate-like shapes. Elemental analysis (%) calcd for $C_{22}H_{16}Mo_{12}N_2O_{40}PS_8$: C 11.07, H 0.68, N, 1.17; found: C 11.60, H 1.14, N 1.26. FT-IR (KBr disc): 3495(br), 3098(m), 1632(m), 1603(w), 1523(w), 1506(w) 1472(w), 1354(w), 1243(w), 1057 (s), 955(s), 860(m), and 789(s) cm^{-1}. UV/Vis-NIR in KBr: absorption at 232, 318, 596, and 992 nm. The former two bands originated from ligand to metal charge transfer (MLCT) in $\{PMo_{12}\}$ and intramolecular transition in the TTFPyH molecule, respectively. Bands at 596 and 992 nm can be attributed to the intramolecular transition of oxidized TTFPyH[15] and intervalence charge-transfer (IVCT) absorption of reduced $[PMo^{V}Mo^{VI}_{11}O_{40}]^{4-}$ clusters,[16] respectively. The band at 992 nm is considered to overlap with that of an intra-dimer transition between TTF^{+}.[7a]

Single-crystal X-ray diffraction analysis[17] was performed using a Rigaku R-AXIS RAPID with graphite monochromated Cu-Kα radiation. The data were collected at 120 K to a maximum 2θ value of 65.0. The structure was determined by direct methods and expanded using Fourier techniques. All calculations were performed using the Crystal Structure crystallographic software package.

Electrical conductivity measurements were performed by DC two probe measurement using single crystals of **1**. Gold paste was utilized for electrodes and electrical contacts were made using gold wires. Temperature dependence and current-voltage (I–V) characteristics were measured under vacuum using a commercially available cryostat with a temperature control system over the range indicated in the main text. The current was monitored with a Keithley 6517 electrometer, with a constant bias voltage ranging between -1 and $+1$ V. Similar experiments for AC conductivity measurements (HP 4194a) were performed using the same single crystal.

Magnetic measurements were performed using a Quantum Design SQUID magnetometer. The temperature dependence of the molar magnetic susceptibility was measured between 22 and 300 K in an external field of 5000 Oe. Powder samples were fixed in polyvinylidene chloride foils for measurements.

Received: June 13, 2014
Published online: July 31, 2014

Keywords: conducting materials · molecular electronics · nanoparticles · polyoxometalates

[1] a) Y. F. Song, R. Tsunashima, *Chem. Soc. Rev.* **2012**, *41*, 7384–7402; b) D.-L. Long, R. Tsunashima, L. Cronin, *Angew. Chem.* **2010**, *122*, 1780–1803; *Angew. Chem. Int. Ed.* **2010**, *49*, 1736–1758; c) A. Müller, F. Peters, M. T. Pope, D. Gatteschi, *Chem. Rev.* **1998**, *98*, 239–272; d) C. L. Hill, *Chem. Rev.* **1998**, *98*, 1–2; e) P. Kögerler, B. Tsukerblat, A. Müller, *Dalton Trans.* **2010**, *39*, 21–36; f) U. Kortz, A. Müller, J. Slageren, J. Schnack, N. S. Dalal, M. Dressel, *Coord. Chem. Rev.* **2009**, *253*, 2315–2327; g) N. Mizuno, M. Misono, *Chem. Rev.* **1998**, *98*, 199–218.

[2] a) J. M. Clemente-Juan, E. Coronado, A. Gaita-Ariño, *Chem. Soc. Rev.* **2012**, *41*, 7464 – 7478; b) N. Casañ-Pastor, L. C. Baker, *J. Am. Chem. Soc.* **1992**, *114*, 10384 – 10401; c) R. A. Prados, M. T. Pope, *Inorg. Chem.* **1976**, *15*, 2547 – 2553; d) C. Sanchez, J. Livage, J. P. Launay, M. Fournier, *J. Am. Chem. Soc.* **1983**, *105*, 6817 – 6823.

[3] J. Lehmann, A. Gaita-Ariño, E. Coronado, D. Loss, *Nat. Nanotechnol.* **2007**, *2*, 312 – 317.

[4] C. Fleming, D.-L. Long, N. McMillan, J. Johnson, N. Bovet, V. Dhanak, N. Gadegaard, P. Kögerler, L. Cronin, M. Kadodwala, *Nat. Nanotechnol.* **2008**, *3*, 229 – 233.

[5] a) D. Velessiotis, N. Glezos, V. Ioannou-Sougleridis, *J. Appl. Phys.* **2005**, *98*, 0845031 – 0845034; b) A. M. Douvas, E. Makarona, N. Glezos, P. Argitis, J. A. Mielczarski, E. Mielczarski, *ACS Nano* **2008**, *2*, 733 – 742.

[6] a) G. Saito, Y. Yoshida, *Bull. Chem. Soc. Jpn.* **2007**, *80*, 1 – 137; b) T. Akutagawa, T. Ohta, T. Hasegawa, T. Nakamura, C. A. Christensen, J. Becher, *Proc. Natl. Acad. Sci. USA* **2002**, *99*, 5028 – 5033; c) R. Tsunashima, Y. Noda, Y. Tatewaki, S.-i. Noro, T. Akutagawa, T. Nakamura, T. Matsumoto, T. Kawai, *Appl. Phys. Lett.* **2008**, *93*, 1731021 – 17310213; d) E. Coronado, C. J. Gómez-García, *Chem. Rev.* **1998**, *98*, 273 – 296; e) L. Ouahab, M. Bencharif, D. Grandjean, *C. R. Acad. Sci. Ser. II* **1988**, *307*, 749 – 755; f) S. Triki, L. Ouahab, J.-F. Halet, O. Peña, J. Padiou, D. Grandjean, C. Garrigou-Lagrange, P. Delhaes, *J. Chem. Soc. Dalton Trans.* **1992**, 1217 – 1227; g) E. Coronado, C. Giménez-Saiz, C. J. Gómez-García, *Coord. Chem. Rev.* **2005**, *249*, 1776 – 1796; h) J. R. Galán-Mascarós, C. Giménez-Saiz, S. Triki, C. J. Gómez-García, E. Coronado, L. Ouahab, *Angew. Chem. Int. Ed. Engl.* **1995**, *34*, 1460 – 1462; *Angew. Chem.* **1995**, *107*, 1601 – 1603.

[7] a) B. A. Scott, S. J. La Placa, J. B. Torrance, B. D. Silverman, B. Welber, *J. Am. Chem. Soc.* **1977**, *99*, 6631 – 6639; b) T. Mori, A. Kobayashi, Y. Sasaki, H. Kobayashi, G. Saito, H. Inokuchi, *Bull. Chem. Soc. Jpn.* **1984**, *57*, 627 – 633.

[8] S. C. Lee, A. Ueda, H. Kamo, K. Takahashi, M. Uruichi, K. Yamamoto, K. Yakushi, A. Nakao, R. Kumai, K. Kobayashi, H. Nakao, Y. Murakami, H. Mori, *Chem. Commun.* **2012**, *48*, 8673 – 8675.

[9] R. Bozio, I. Zanon, A. Girlando, C. Pecile, *J. Chem. Phys.* **1979**, *71*, 2282 – 2293.

[10] Similar orbital energies between TTFPy and $[PMo^{VI}_{12}O_{40}]^{3-}$ are only expected between the HOMO of TTFPy and the LUMO of the cluster anion. The redox potentials of these orbitals in the solution phase show the LUMO of $[PMo^{VI}_{12}O_{40}]^{3-}$ is higher than HOMO of TTFPy by ca. 0.2 eV, however these two orbitals do not overlap (see Supporting Information). The HOMO–LUMO gap of $[PMo^{VI}_{12}O_{40}]^{3-}$ is observed at 232 or 318 nm. Namely, the orbital energies of the O atoms are 4–5 eV below the HOMO of TTFPy.

[11] J. Han, M. Shen, W. Cao, A. M. R. Senos, P. Q. Mantas, *Appl. Phys. Lett.* **2003**, *82*, 67 – 69.

[12] a) D. Yu, C. Wang, B. L. Wehrenberg, P. Guyot-Sionnest, *Phys. Rev. Lett.* **2004**, *92*, 2168021 – 2168024; b) R. Parthasarathy, X.-M. Lin, H. M. Jaeger, *Phys. Rev. Lett.* **2001**, *87*, 1868071 – 1868074; c) T. B. Tran, I. S. Beloborodov, X. M. Lin, T. P. Bigioni, V. M. Vinokur, H. M. Jaeger, *Phys. Rev. Lett.* **2005**, *95*, 0768061 – 07680614; d) Y. Tatewaki, Y. Noda, T. Akutagawa, R. Tsunashima, S.-i. Noro, T. Nakamura, H. Hasegawa, S. Mashiko, J. Becher, *J. Phys. Chem. C* **2007**, *111*, 18871 – 18877; e) Y. Noda, S.-i. Noro, T. Akutagawa, T. Nakamura, *Phys. Rev. Lett.* **2010**, *82*, 2054201 – 2054206; f) T. Sugawara, M. Minamoto, M. M. Matsushita, P. Nickels, S. Komiyama, *Phys. Rev. B* **2008**, *77*, 2353161 – 2353167; g) J. M. Wessels, H.-G. Nothofer, W. E. Ford, F. Wrochem, F. Scholz, T. Vossmeyer, A. Schroedter, H. Weller, A. Yasuda, *J. Am. Chem. Soc.* **2004**, *126*, 3349 – 3356; h) R. Parthasarathy, X.-M. Lin, H. M. Jaeger, *Phys. Rev. Lett.* **2001**, *87*, 1868071 – 1868074.

[13] G. Orsini, V. Tricoli, *J. Mater. Chem.* **2011**, *21*, 14530 – 14542.

[14] L. Wang, B. Zhang, J. Zhang, *Inorg. Chem.* **2006**, *45*, 6860 – 6863.

[15] a) A band was observed at 772 nm (in CH_2Cl_2/CH_3CN) upon both oxidation and protonation of a similar compound of 2,3-dimethylthio-6-pyridyl-tetrathiafulvalene, see Ref. [15b]; b) Q. Y. Zhu, Y. Liu, W. Lu, Y. Zhang, G. Q. Bian, G. Y. Niu, J. Dai, *Inorg. Chem.* **2007**, *46*, 10065 – 10070.

[16] a) $[P\,Mo^{V}Mo^{VI}_{11}O_{40}]^{4-}$ in acetonitrile shows bands at 342 and 750 nm with a shoulder at 1050 nm, see Ref [16b]; b) H.-R. Sun, S.-Y. Zhang, J.-Q. Xu, G.-Y. Yang, T.-S. Shi, *J. Electroanal. Chem.* **1998**, *455*, 57 – 68.

[17] $(TTFPyH)_2[PMo^{V}Mo^{VI}_{11}O_{40}]\cdot n\,H_2O$ (**1**): $C_{22}H_{16}Mo_{12}N_2O_{46}PS_8$ for $n = 6$, $M_r = 2483.18\ g\,mol^{-1}$, plate like crystal, $0.106 \times 0.134 \times 0.170\ mm^3$, $T = 173(2)$ K, triclinic, space group $P\bar{1}$, $a = 11.663(11)$, $b = 11.750(12)$, $c = 12.304(10)$ Å, $\alpha = 61.81(4)$, $\beta = 70.33(4)$, $\gamma = 78.41(6)°$, $V = 1398(2)$ Å^3, $Z = 1$, $\rho = 2.950\ g\,cm^{-3}$, $F(000) = 1177$, 11445 reflections measured, 4895 unique ($R_{int} = 0.0530$), 430 refined parameters, $R1 = 0.0570$, $wR2 = 0.1497$. Six numbers of crystalline water molecules were crystallographically identified and their six number of O atoms were included to crystallographic composition shown above. CCDC 1008211 (**1**) contains the supplementary crystallographic data for this paper. These data can be obtained free of charge from The Cambridge Crystallographic Data Centre via www.ccdc.cam.ac.uk/data_request/cif.

